石油科学通报
Petroleum Science Bulletin

超临界 CO_2 压裂诱导裂缝机理研究综述

周大伟，张广清*

中国石油大学(北京)石油工程学院，北京 102249
* 通信作者, zhangguangqing@cup.edu.cn

收稿日期: 2019−11−22
国家杰出青年科学基金(51925405)、国家自然科学基金面上项目(51774299) 和国家科技重大专项(2016ZX05046−04, 2016ZX05050, 2017ZX05069) 联合资助

摘要 超临界二氧化碳(SC-CO_2)压裂改造非常规储层具有提高油气产量、储层无污染、节约水资源、埋存CO_2等优点，受到了工业界和学术界的广泛关注。本文综述了目前室内SC-CO_2压裂实验方法、裂缝起裂扩展特征与机理，以及存在的问题并给出建议。SC-CO_2与岩石的“热(T)—流(H)—力(M)—化(C)”多场耦合作用机理为诱导应力和弱化断裂性质两方面。诱导应力方面包括：SC-CO_2低黏度和高扩散性导致的孔隙压力场和热应力场，共同降低有效应力并诱发天然裂缝的剪切破坏(TH-M)；SC-CO_2相变释放的能量以冲击载荷和热应力的形式促进裂缝动态扩展(TH-M)。弱化断裂性质方面包括：零表面张力的SC-CO_2可进入微裂纹尖端，降低裂缝扩展所需的缝内净压力(H-M)；SC-CO_2吸附在微裂纹表面，降低裂缝失稳扩展所需的临界应力(C-M)。因此，SC-CO_2压裂易于形成以I-II混合型破坏为主的多裂缝，适合改造裂缝性致密储层。未来应积极开展SC-CO_2三维裂缝扩展实验模拟，进行裂缝特征重构和定量评价，利用理论模型和数值模拟研究方法，实现研究尺度的升级，加快SC-CO_2压裂工业应用进程。

关键词 SC-CO_2压裂；裂缝形成机理；实验研究；THMC耦合；非常规油气

A review of mechanisms of induced fractures in SC-CO_2 fracturing

ZHOU Dawei, ZHANG Guangqing

College of Petroleum Engineering, China University of Petroleum-Beijing, Beijing 102249, China

Abstract In unconventional reservoir stimulation, Supercritical (SC) CO_2 fracturing can not only increase oil/gas production, minimize formation damage and conserve water resources, but also promote CO_2 geological storage, which draws broad attention in both industry and academia. This work reviewed the current studies with respect to experimental techniques, characteristics and mechanisms of fracture initiation and propagation, and related existing problems and suggestions in SC-CO_2 fracturing. The mechanisms of coupled thermo-hydro-mechanical-chemical (THMC) processes between SC-CO_2 and rockare induced stress and weakened fracture toughness. The induced stress includes the thermal stress and pore pressure field induced by the low viscosity and high diffusionof SC-CO_2, which can lower the effective stress and even create shear failure (TH-M effects). Thedynamic load and thermal stress created by the SC-CO_2 phase change can enhance micro-fracture initiation and propagation (TH-M effects). The weakened fracture toughness includes SC-CO_2 of zero surface tension, tending to penetrate into the micro-cracks to lower fracture net pressure for crack growth (H-M effects). CO_2 adsorption can lower the surface energy of rock and this in turn reduces the critical stress for crack growth (C-M effects). Therefore, SC-CO_2 fracturing tends to create multiple fractures characterized by

引用格式：周大伟，张广清. 超临界CO_2压裂诱导裂缝机理研究综述. 石油科学通报，2020, 02: 239−253
ZHOU Dawei, ZHANG Guangqing. A review of mechanisms of induced fractures in SC-CO_2 fracturing. Petroleum Science Bulletin, 2020, 02: 239-253. 10.3969/j.issn.2096-1693.2020.02.021

I-II type failure, which can be applied for stimulation of fracturedtight reservoirs. So, in the future, it will be necessary to conduct SC-CO_2 fracturing experiments, to be used to reconstruct and evaluate the induced 3D fractures. The research scale is upgraded with the theoretical and numerical models to accelerate the process of SC-CO_2 fracturing in the field.

Keywords SC-CO_2 fracturing; fracture mechanism; experimental study; THMC coupling; unconventional reservoirs

doi: 10.3969/j.issn.2096-1693.2020.02.021

0 前言

随着世界范围内温室效应日趋严重，预计在 2050 至 2055 年之间全球CO_2总排放量会超过临界值 3.67 万亿吨，使全球平均温度上升约 2 ℃，严重威胁全球气候[1]。目前，人类除了开发新能源(太阳能、核能、生物能等)和清洁能源(天然气、地热等)降低CO_2排放量外，还采用CO_2埋存(CCS)、CO_2驱油(CO_2−EOR)、CO_2压裂和CO_2增强型地热开采(CO_2−EGS)等措施降低大气中CO_2含量。考虑到水力压裂技术存在产量递减快和环境污染等问题，CO_2压裂以其无水项、无残留等特点，成为目前主要的商业化无水压裂技术。CO_2压裂具有保护环境、节约水资源、提高油气产量、埋存CO_2的优点，在非常规油气储层(页岩气[2]、页岩油[3]、煤层气[4]等)增产开发中具有广阔的应用前景。

CO_2压裂技术是以CO_2作为压裂液添加剂或携砂液的压裂增产工艺，可分为CO_2增能压裂、CO_2泡沫压裂和液态(L−)或超临界态CO_2(SC−CO_2)压裂[2]。CO_2干法压裂技术是采用 100%的低温 L−CO_2(P=1.406 MPa，T=−34.4 ℃)混合支撑剂进行压裂的工艺方法，CO_2以液态形式进入储层[5]。1981 年 L−CO_2加砂压裂概念首先被提出，并成功应用于加拿大 Glauconite 砂岩油藏压裂增产，储层无伤害且明显提高油气产量[6]。从 2005 年开始，国内长庆油田、中原油田、吉林油田和延长油田针对储层的压力低、水敏严重、用水量大、压裂液返排慢等问题，相继开展液态CO_2压裂，取得良好增产效果[2,7−13]。相对于 L−CO_2，SC−CO_2的密度接近液体、黏度接近气体、扩散系数比液体大、具有很强的溶剂化能力和良好的传质等物理特性。SC−CO_2破岩最早应用于钻井提速，发现 SC−CO_2射流破岩的门限压力比水射流低 50%以上[14]。随着研究的深入，研究者发现 SC−CO_2造缝能力要远大于 L−CO_2，具有很好的压裂应用前景[15]。L−CO_2压裂由于只有部分阶段CO_2转化为超临界态驱动裂缝扩展，没有充分发挥 SC−CO_2的造缝能力。SC−CO_2压裂技术采用的CO_2初始温度较高，确保CO_2在井筒内完全转化为超临界状态(例如：排量为 2 m^3/min，井口加热CO_2到−10 ℃，达到 2000 m 的井底时其温度约为 35 ℃[5])，最终CO_2以超临界状态进入储层。因此，SC−CO_2压裂的缝内CO_2始终以超临界态形式驱动裂缝扩展。

2010 年以后，随着水平井体积压裂技术的发展，非常规油气(页岩油气、超低渗致密砂岩等)资源得到商业化开发，学者开始论证 SC−CO_2压裂技术改造非常规油气资源的可行性。2012 年以后，大量学者通过开展不同的岩性(页岩、致密砂岩、人工试件)、储层条件(应力状态、温度)、施工条件(排量)下室内 SC−CO_2压裂实验，对比水基、油基及其它气体(He, N_2等)的压裂效果，发现 SC−CO_2压裂具有破裂压力低、易于形成多裂缝且裂缝迂曲等特点[16−18]。基于室内压裂实验研究，学者分别采用有限元(FEM)[19−20]和离散元(UDEC)[21]等数值方法对比研究CO_2与其它流体压裂的异同。同时，学者建立相应的计算模型研究表面张力[22]、流体压缩性[23]、热应力[24]等对CO_2诱导裂缝扩展的影响。目前，已有综述类文章[2,5,8,15,25−32]分析CO_2压裂的优缺点，论证其改造非常规储层的可行性，并指出CO_2压裂适合改造渗透率低和地应力差大的裂缝性非常规储层。

截止目前，水基压裂液仍作为非常规储层改造的主要压裂液介质，存在伤害储层、污染地下水、返排液处理难度大、用水量巨大等缺点[33−35]。CO_2压裂由于施工工艺和成本原因，并未大规模应用于现场，尤其是 SC−CO_2压裂对设备要求更为苛刻，其现场应用难度更大。SC−CO_2压裂研究主要集中于室内实验和理论研究两方面，探究 SC−CO_2压裂裂缝扩展机理。本文从 SC−CO_2压裂机理研究角度出发开展 4 方面的论述：(1)SC−CO_2压裂实验模拟方法；(2)SC−CO_2压裂裂缝起裂与扩展特征；(3)SC−CO_2诱导裂缝扩展机理；(4)SC−CO_2压裂机理研究存在的问题及建议。

1 SC-CO_2压裂实验模拟方法

如图 1 所示，非常规油气储层埋深一般为 2000~7000 m[36]，其温度、压力均已超过CO_2的临界

条件(P=7.38 MPa, T=31.1 ℃)，因此CO_2压裂实验模拟需达到超临界状态条件。

目前，室内SC−CO_2压裂模拟一般采用常规水力压裂加载装置[38]，将水基压裂液注入系统改为CO_2注入系统，并在注入端位置增添加热装置(图 2)。CO_2首先进入冷却装置完全转化为液态，从而降低其压缩系数，提高CO_2泵增压效率，增压至临界压力(P=7.38 MPa)以上。然后L−CO_2流经加热装置，加热到临界温度(T=31.1 ℃)以上，最终CO_2以超临界状态进入试件[39−40]。为了模拟储层应力和温度条件，围压腔可提供孔压和温度，扁千斤可施加三向地应力。

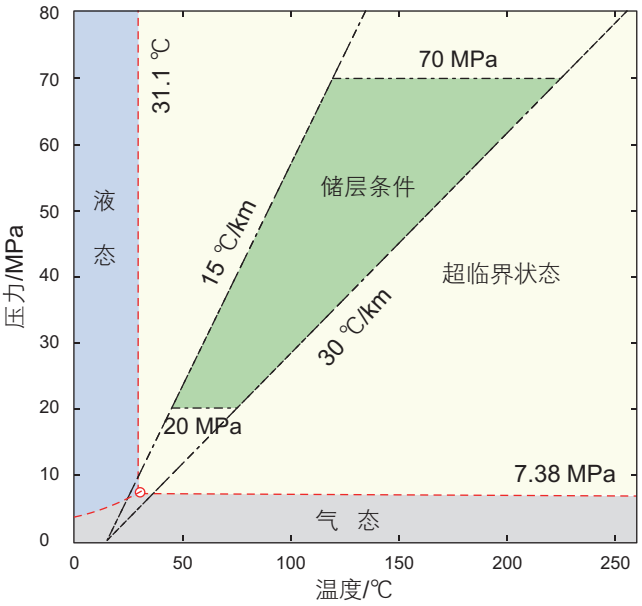

图 1 储层条件下SC-CO_2相态分布图(绿色部分)(取储层深度为 2~7 km[36]，地表平均温度为 15 ℃，地温梯度为 15~30 ℃/km，地层压力梯度为 1 MPa/km[37])

Fig. 1 The distribution of CO_2 phase diagram under the reservoir conditions characterized with green part (the depth of reservoir is 2~7 km, the surface temperature is 15 ℃, the geothermal gradient is 15~30 ℃/km, and the formation pressure gradient is 1 MPa/km[37])

2 SC-CO_2 诱导裂缝起裂与扩展特征

为了增大储层的改造体积(SRV)，人们不断尝试新的压裂方法。常规水力压裂往往形成单一裂缝(图 3(a))，其改造效果有限；爆炸压裂产生的高应力、高加载速率导致近井地带形成塑性压实区，裂缝扩展距离有限，降低了岩石的渗透率(图 3(b))[41]；高能气体压裂利用推进剂或火药燃烧产生高温高压气体作用在井壁岩石上，进而产生多裂缝，但是由于其现场可操作性和安全性问题，并未得到推广(图 3(c))[9,42]；气体压裂(CO_2、N_2等)容易沟通天然裂缝[31]，增大储层的SRV[43](图 3(d))，其中CO_2压裂现场操作可行性高且增产效果明显，因此得到了广泛关注。

目前，室内SC−CO_2压裂模拟试件类型包括两类：圆柱和立方体。圆柱试件可施加两向偏应力($\sigma_1>\sigma_2=\sigma_3$)，往往以裸眼方式起裂；立方体试件可施加三向应力($\sigma_1>\sigma_2>\sigma_3$)，以裸眼和射孔(割缝)方式起裂。压裂模拟试件主要有天然露头(花岗岩、页岩、致密砂岩、煤岩等)和类岩石材料(人工水泥试件、有机玻璃(PMMA))。目前SC−CO_2压裂实验最高温度达 300 ℃[44]，最大施加应力达 52.5 MPa[45]。如表 1 所示，本文总结了已有不同相态CO_2压裂实验的试件类型及尺寸、实验条件、研究方法和结论，通过分

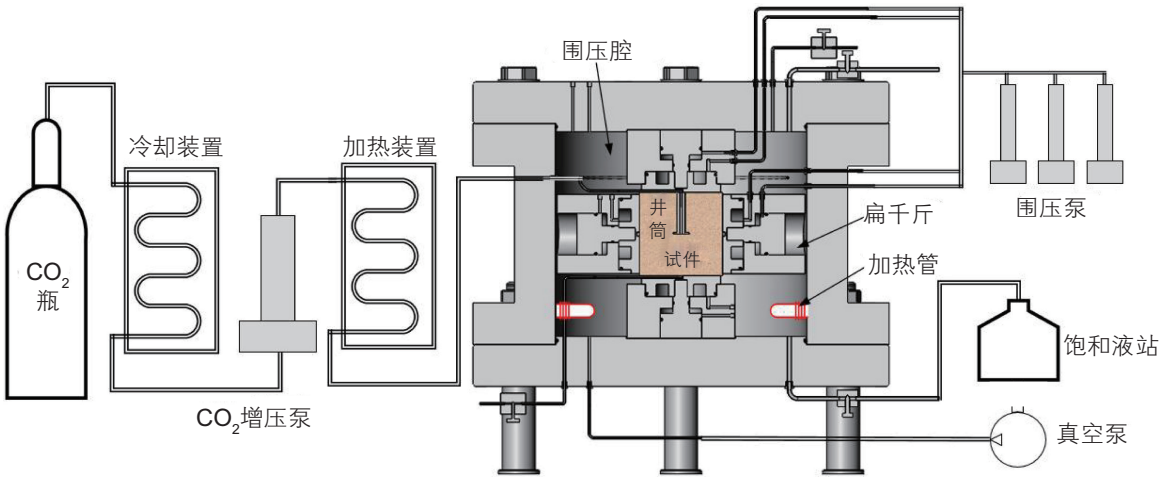

图 2 SC-CO_2 压裂系统示意图

Fig. 2 The sketch of SC-CO_2 fracturing system

析注入压力、宏观/微观裂缝形态、井底或缝内温度、声发射及声波特征等数据，研究CO_2诱导裂缝起裂及扩展特征，并分析其形成机理。

压裂改造效果受到地质(地应力状态、储层岩石性质等)和工程(完井及射孔方式、压裂液类型及排量)因素影响[59]，其中破裂压力和裂缝形态可表征各因素的影响规律。随着压裂液黏度的降低($v_{H_2O}>v_{L-CO_2}>v_{SC-CO_2}$)，破裂压力急剧降低(图 4(a))，易形成裂缝网

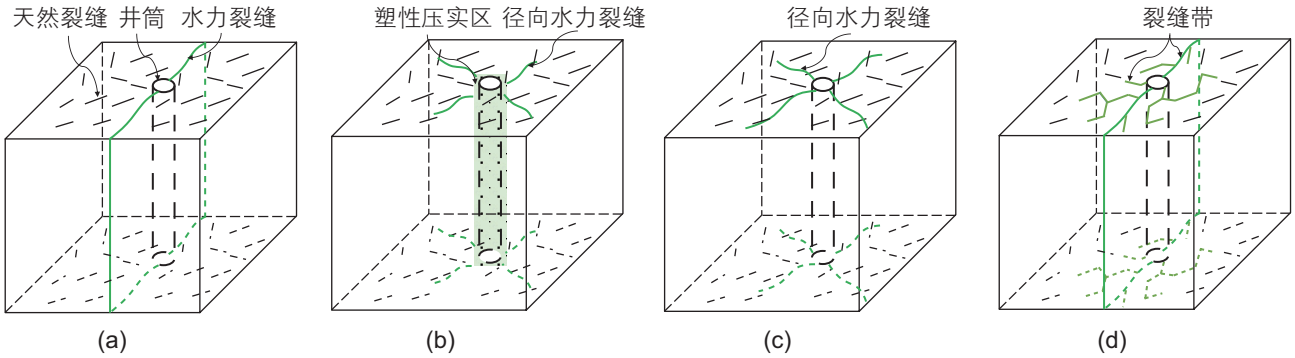

图 3 (a)水力压裂;(b)爆炸压裂;(c)高能气体压裂和(d)气体压裂形成的裂缝形态对比((a),(b),(c)修改自 Safari et al.[41])

Fig. 3 Comparison of fracture patterns form a variety of techniques (a) hydraulic (b) explosive (c) high energy and (d) gas fracturing ((a),(b),(c) modified from Safari et al.[41])

表 1 目前CO_2压裂实验结果分析总结

Table 1 A review of CO_2 fracturing

试件类型	尺寸/cm	实验条件	主要分析方法	主要研究结论	参考文献
花岗岩和凝灰岩	15×15×15	σ_1, σ_2, σ_3=5, 3, 1; T=40; Q_{CO_2}=10,50,100; F_f: SC-CO_2, 水	3D裂缝形态; 注入压力−温度曲线	低黏度和弱结构有利于SC-CO_2诱导分支裂缝	Kizaki et al.(2012)[15]
花岗岩	17×17×17	σ_1, σ_2, σ_3=6, 4, 3; T=45; Q_{CO_2}=10; F_f: SC-CO_2, 水, 油	AE信号; 微观裂缝形态	SC-CO_2诱导裂缝迂曲度大; 主裂缝周围有大量分支裂缝; 易于发生剪切破坏	Ishida et al.(2012)[14], Chen et al.(2015)[46]
页岩	D=2.5 L=5	σ_a, σ_c=0~35,10~25; 室温条件; Q_{CO_2}=5; F_f: 水, L-CO_2, N_2	P_b分析; 裂缝面粗糙度和分形维数	L-CO_2的P_b最高; L-CO_2诱导裂缝面粗糙度、分形维数大	Li et al.(2016)[16]
页岩	20×20×20	σ_1=12, σ_2=9, 10, σ_3=6, 8, 10; Q_{CO_2}=30; T=18,60; F_f: 水, L/SC-CO_2	裂缝CT扫描; AE信号	SC-CO_2的P_b比水的低50%以上; 孔压可降低P_b; SC-CO_2易于沟通天然裂缝和层理	Zhang et al.(2017)[17]
页岩	20×20×20	σ_1, σ_2, σ_3=14.5~20.7, 11~14.5, 7.6~14.5; Q_{CO_2}=40,80; T=50~55; F_f: 滑溜水, 气态CO_2, SC-CO_2	注入压力−温度曲线; 主动声波P和S波; 压降曲线	SC-CO_2膨胀性和热应力促使裂缝扩展; SC-CO_2的低黏度和天然裂缝是降低P_b的关键	Wang et al.(2017)[47]
花岗岩	/	距地面约50 m的隧道内的含水花岗岩, 井深为7.24~7.4 m; Q_{CO_2}=50; T=35; F_f: SC-CO_2	AE信号; 井底温度−压力变化	SC-CO_2容易沿着天然节理扩展	Ishida et al.(2017)[48]
煤岩	D=3.8, L=7.6	σ_a, σ_c=6,8; T=25; Q_{CO_2}=90; F_f: L-CO_2, 水	AE信号; P_b和裂缝形态	L-CO_2的P_b比水的小19.6%; L-CO_2的低黏度和膨胀性促使产生多裂缝	Sampath et al.(2018)[49]

续表

试件类型	尺寸/cm	实验条件	主要分析方法	主要研究结论	参考文献
煤岩	10 × 10 × 10	σ_1=14, 16, σ_2=12,14, σ_3=10, 12; Q_{CO_2}=20;T=50; F_f: SC-CO_2, 水	裂缝形态；P_b分析	SC-CO_2 产生复杂的交叉裂缝，裂缝宽小	王磊等(2019)[50]
页岩	D=10, L=20	σ_a, σ_c=25~52.5,7.47~15.68; 梯级恒压注入；T=40；F_f：SC-CO_2, 水	AE信号；裂缝CT扫描	SC-CO_2 易于沿着天然裂缝或弱结构面延伸裂缝，并发生部分剪切破坏	Jiang et al. (2018)[45]
页岩	D=10, L=16	σ_a, σ_c=15,0~15; Q_{CO_2}=50;T=45；F_f: SC-CO_2	注入压力曲线；裂缝面3D扫描分析粗糙度和迂曲度	SC-CO_2 压裂易形成弯曲裂缝和多分支缝	Zhao et al. (2018)[51]
致密砂岩	30 × 30 × 30	σ_1, σ_2, σ_3=25, 20(15), 10; Q_{CO_2}=20, 50; T=80; F_f: SC-CO_2, 滑溜水，瓜尔胶压裂液	AE震源机制；裂缝CT扫描	SC-CO_2 降低P_b；诱发层理或天然裂缝的剪切破坏	Zou et al. (2018)[52]
致密砂岩	8 × 8 × 10	σ_1, σ_2, σ_3=15, 15 或 10, 7; Q_{CO_2}=5, 20, 50;T=60,20; F_f：L/SC-CO_2, 滑溜水	裂缝形态；P_b分析	SC-CO_2 降低P_b；诱导复杂裂缝	叶亮等(2018)[53]
页岩和煤岩	10 × 10 × 10	σ_1, σ_2, σ_3=25~28, 5~18, 5~8; Q_{CO_2}=60, 120;室温；F_f: L-CO_2, 水	裂缝CT扫描；P_b分析	L-CO_2 诱导已有裂缝发生剪切破坏，产生分支裂缝	Deng et al. (2018)[54]
花岗岩	D=2.25, L=4.5	σ_c=σ_a=5~40; T=50~300; Q_{CO_2}=30; F_f：SC-CO_2, 水	裂缝CT密度；CO_2 进出口压力变化	高温作用可降低P_b；易产生分支生裂缝；论证了SC-CO_2 进行地热开采的可行性	Isaka et al. (2019)[44]
页岩	D=5, L=10	σ_a, σ_c=10, 0; Q_{CO_2}=30; F_f: SC-CO_2, 水	裂缝SEM扫描；裂缝迂曲度和裂缝密度	层理影响P_b与裂缝形态；SC-CO_2 沟通有机质孔与微裂缝，增大渗透率	He et al. (2019)[55]
PMMA	10.1 × 10.1 × 10.1 和 12.1 × 12.1 × 12.1	σ_1, σ_2, σ_3=5, 5, 0; T=60; Q_{CO_2}=25; F_f：CO_2, He, N_2, Ar, SF_6, H_2O	裂缝3D形态	L-CO_2 同SF_6，H_2O，He一样产生简单裂缝	Alpern et al. (2012)[56]
PMMA	20 × 20 × 10	σ_1, σ_2, σ_3=1.8, 1.8, 0; T=60; Q_{CO_2}=2; F_f：SC-CO_2 和水	裂缝扩展可视化	SC-CO_2 相变导致裂缝动态扩展形成复杂裂缝	Zhou et al. (2018)[40]
水泥试件	30 × 30 × 30	σ_1, σ_2, σ_3=30, 28, 24; T=25~100; Q_{CO_2}=26.7, 40; F_f: L-CO_2	井底及缝内压力－温度曲线；裂缝形态	建立了考虑热应力的CO_2 压裂起裂及扩展理论模型；低温CO_2 热应力促使产生分支裂缝	Zhou et al. (2019)[18]
水泥试件	30 × 30 × 30	σ_1, σ_2, σ_3=23, 21, 13~19; Q_{CO_2}=26; T=45; F_f: SC-CO_2, 瓜尔胶压裂液	AE信号；裂缝断裂角分析	SC-CO_2 压裂裂缝为非连续动态扩展，诱导剪切破坏，形成分支裂缝	Zhou et al. (2018)[39]; Zhou et al. (2019)[57]
水泥试件	30 × 30 × 30	σ_1, σ_2, σ_3=10.5, 9.8, 8.5; T=60; F_f: SC-CO_2, 水	AE信号；裂缝形态	射孔角度越大，SC-CO_2 诱导裂缝越复杂；在高射孔角度下，应力状态对SC-CO_2 压裂影响较小	Chen et al. (2019)[58]

注：D、L为圆柱试件的直径和长度(cm)，σ_c、σ_a为圆柱试件所受径向和轴向应力(MPa)，T为实验温度(℃)，σ_1, σ_2, σ_3 为三向主应力(MPa)，Q为注入速率(mL/min)，P_b为破裂压力，F_f代表压裂液类型。

络(图 4 (b))。

目前，学者主要从SC−CO_2的黏度等物性特征研究裂缝扩展特征与力学机理，主要认识有：(1)SC−CO_2的破裂压力均比水、L−CO_2、油以及其它气体(N_2、He等)的低，最大降幅达 50%以上；(2)SC−CO_2容易形成分支裂缝、多裂缝以及迂曲裂缝，且裂缝面粗糙、缝宽小；(3)有效应力、热应力、表面张力等是控制裂缝扩展的主要力学因素。

3 SC-CO_2 诱导裂缝扩展机理

SC−CO_2的特殊物理化学性质，使其与储层岩石—流体之间THMC耦合作用强烈，如图 5 所示。以下将分别叙述SC−CO_2流体诱导裂缝扩展的 4 个机理：(1)热应力和孔压降低有效应力及诱发剪切破坏(TH−M)；(2)零表面张力降低裂缝扩展所需缝内净压力(H−

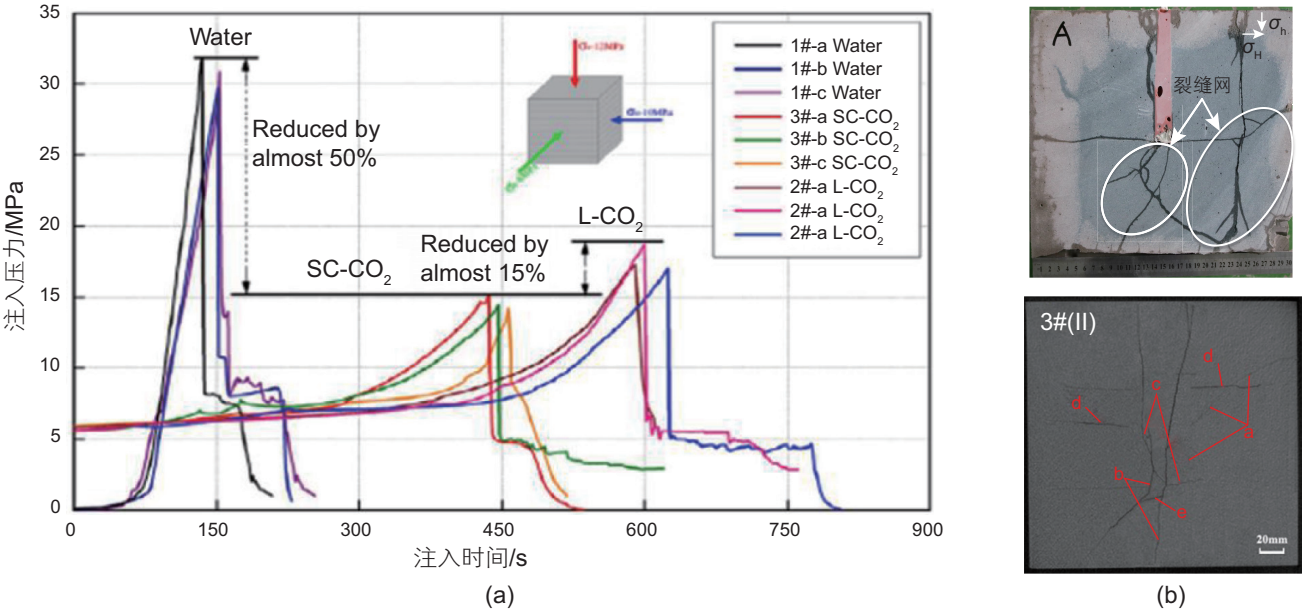

图 4 (a) 页岩SC-CO_2，L-CO_2和水基压裂液的破裂压力比较[17]和 (b) 人工水泥试件[39]、页岩[17]裂缝形态

Fig. 4 (a) The comparison of breakdown pressure using SC-CO_2, L-CO_2 and waterof shale[17] and (b) SC-CO_2 induced fractures of cement specimen[39] and shale[17]

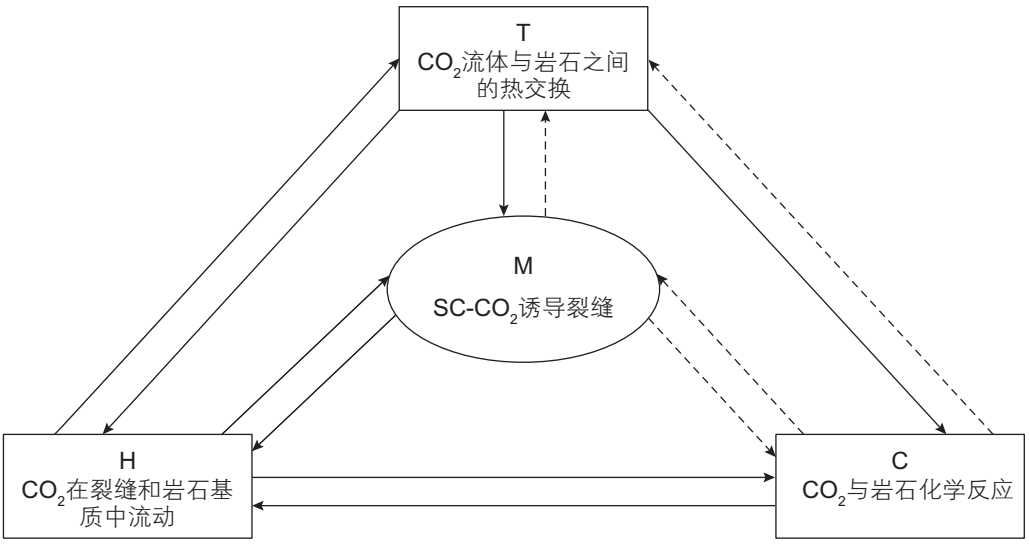

图 5 SC-CO_2压裂中热(T)−流(H)−力(M)−化(C)耦合过程(实线表示强耦合，虚线为弱耦合)

Fig. 5 Coupled thermo-hydro-mechanical-chemical (THMC) processes in the SC-CO_2 fracturing. The solid line is the strong coupling and the dashed line is the weak coupling

M)；(3)吸附降低裂缝扩展的临界应力(C−M)；(4)局部相变促进裂缝动态扩展(HT−M)。其中(1)和(4)为SC−CO_2 诱导应力，(2)和(3)为SC−CO_2 弱化断裂性质。

3.1 热应力和孔压降低有效应力及诱发剪切破坏

裂缝内低温CO_2和储层岩石之间温差产生的热应力，降低了裂缝面上的有效正应力，有助于裂缝起裂与扩展，例如在CO_2开采Salah页岩气时井底CO_2与储层温差达40 ℃，使破裂压力降低了1.5~5 MPa[60]。如图6所示，孔弹性条件下，孔隙压力作用效果类似于热应力，裂缝周围压裂液滤失形成的孔隙压力场大于热应力场，垂直和平行于裂缝方向的热应力$\Delta\sigma_{hT}$，$\Delta\sigma_{HT}$分别为[61]：

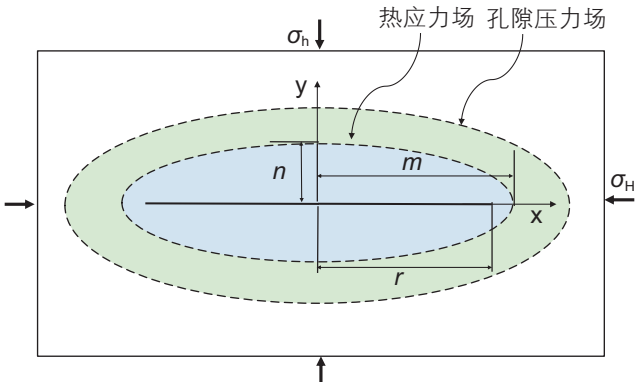

图6 流体诱导裂缝周围热应力场和孔隙压力场分布，*r*为裂缝半长，*m*, *n*分别为冷却区长半轴和短半轴长度(修改自Perkins和Gonzalez[61])

Fig. 6 The distribution of thermal stress and pore pressure around the fluid-driven fracture, *r* is the half fracture length; *m* and *n* are major and minor semiaxis of the elliptical cool region (modified from Perkins and Gonzalez[61])

$$\Delta\sigma_{hT}=\frac{\alpha_T E\Delta T\left(n/m\right)}{\left(1-\nu\right)\left(1+n/m\right)} \tag{1a}$$

$$\Delta\sigma_{HT}=\frac{\alpha_T E\Delta T}{\left(1-\nu\right)\left(1+n/m\right)} \tag{1b}$$

式中：α_T为热膨胀系数，℃$^{-1}$；E为弹性模量，MPa；ΔT为温度变化量，℃；ν为泊松比，无量纲。

由公式(1a)和(1b)可知，随着裂缝的扩展(即n/m减小)[62]，CO_2引起储层岩石的热应力$\Delta\sigma_{HT}$递减速度大于$\Delta\sigma_{hT}$，导致水平有效应力$\sigma_h'\geqslant\sigma_H'$，即初始水平应力方向发生偏转，进而形成垂直于初始裂缝的分支裂缝(图7(a))，该分支裂缝主要以拉伸破坏为主。

SC−CO_2的黏度远低于水(例如，当P=30 MPa，T=60 ℃时，$v_{SC-CO_2}=1/6v_{H_2O}$)，使其易于进入天然裂缝或岩石颗粒边界，从而张开和错动不连续面[29,47,54,63]。Chen[46]研究SC−CO_2压裂花岗岩微观裂缝和AE震源机制，发现颗粒边界处存在明显剪切破坏。2017年日本学者[48]开展现场SC−CO_2压裂花岗岩实验，AE监测表明诱导裂缝易于沿着天然节理扩展。Deng[54]通过页岩和煤岩的L−CO_2和水力压裂实验，指出高应力差条件下L−CO_2容易激活天然裂缝发生剪切破坏，在天然裂缝尖端形成马尾状裂缝[64]，进而贯通邻近裂缝(图7(b))。SC−CO_2低黏度和初始应力差是影响裂缝性储层改造的关键因素，SC−CO_2通过滤失作用改变天然裂缝内部流体压力分布，初始应力差决定了天然裂缝发生剪切破坏的动力大小，两者共同作用激活天然裂缝。

剪切破坏不仅能增大非常规油气[65]和增强型地热系统(EGS)[66]的储层改造体积，而且还能大幅度提高

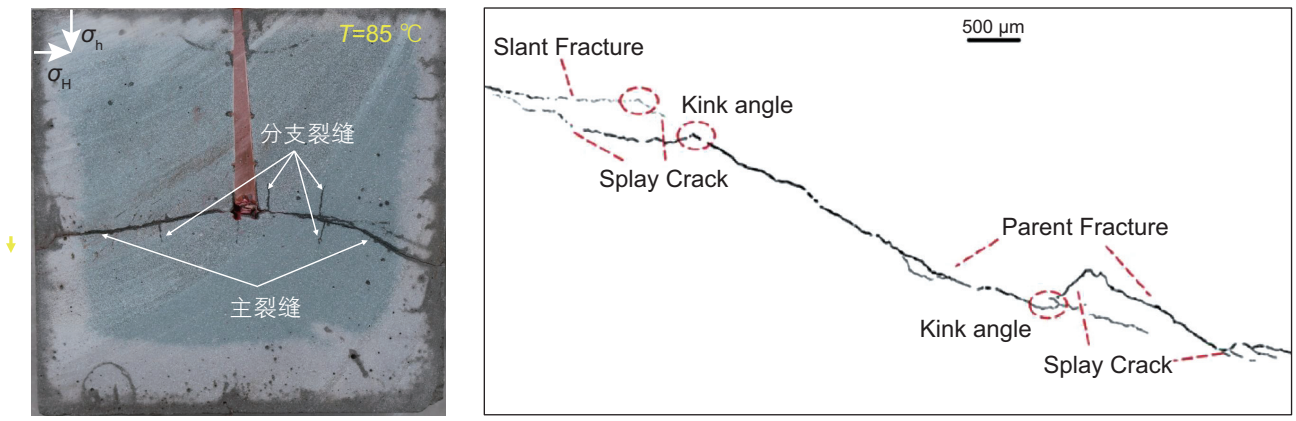

图7 (a) SC-CO_2在主裂缝周围产生分支裂缝[18]；(b)L-CO_2诱导剪切破坏沟通天然裂缝[54]

Fig. 7 (a) Branching fractures are induced by SC-CO_2 around main fracture[18] and (b) the natural fracture connection is created by the shear failure in L-CO_2 fracturing[54]

裂缝的导流能力[67]。根据不同的地质和工程条件，水力压裂过程中存在拉伸(I型)、剪切(II型)以及拉伸—剪切(I−II型)混合破坏。对于均匀连续介质储层的水力压裂来说，人工裂缝以I型破坏为主，裂缝的张开位移D_n随着油气生产逐渐减小甚至完全闭合，导致裂缝的导流能力急剧降低(图 8(a))；对于裂缝性储层的水力压裂来说，当缝内压力不足以张开天然裂缝时，天然裂缝以II型破坏为主，形成剪切位移D_s(图 8(b))，当缝内压力增大时，天然裂缝以I−II混合型破坏为主，产生张开位移D_n和剪切位移D_s(图 8(c))，导致裂缝自支撑且具有高导流能力[43,68]。

3.2 零表面张力降低裂缝扩展所需缝内净压力

压裂液类型及状态是影响裂缝扩展的重要因素，其中流体表面张力决定了压裂液能否进入微裂缝尖端，从而促进微裂纹的扩展。对于非常规致密储层来说，不可忽略毛管力对岩石基质和裂缝中流体流动的影响[69−70]。临界侵入压力P_c为流体克服毛管力进入岩石孔隙所需的压力[22,71]，可由半经验Leveret方程J求解[72]：

$$J=\frac{P_c}{\sigma_s}\sqrt{\frac{k}{\varnothing}} \tag{2}$$

式中：k为渗透率，μm²；$\varnothing$为孔隙度，无量纲；σ_s为压裂液与储层流体之间的表面张力，MPa；对于特定的岩石，J、k、$\varnothing$均为已知常数，P_c与流体表面张力σ_s呈正比关系。

如图 9 所示，压裂液前缘与裂缝尖端之间存在干燥区域称为压裂液滞后(fluid lag)[73−74]。当硬币状水力裂缝准静态扩展时，考虑压裂液滞后影响的裂缝起裂条件[75]：

$$K_{IC}=\frac{2}{\pi}\left[P_f\sqrt{\pi r}-(\sigma_n+P_f)\sqrt{2\pi\lambda}\right] \tag{3}$$

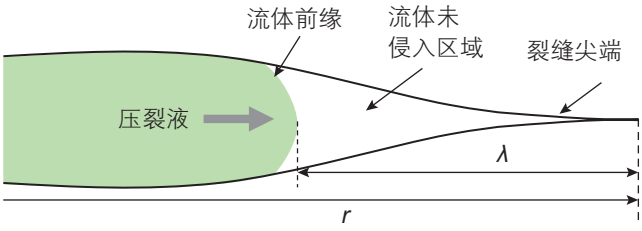

图 9 线弹性断裂条件下水力裂缝尖端区域示意图

Fig.9 The diagram of fracture tip in hydraulic fracturing under LEFM condition

式中：K_{IC}为断裂韧性，MPa$\sqrt{\text{m}}$；P_f为缝内压力，MPa；σ_n为裂缝面上的正应力，MPa；r为裂缝半径，m；λ为滞后区域长度，m。

SC−CO_2的表面张力为零，远小于水和L−CO_2的表面张力(σ_{s,H_2O}=50~70 mN/m，$\sigma_{s,\ L-CO_2}$=40~72 mN/m[76])。由公式(2)，SC−CO_2的临界侵入压力为 0，因此SC−CO_2在泵压的作用下能进入任何大于CO_2分子直径的微裂缝尖端(图 10)。此时，SC−CO_2缝内压力作用长度为$r(\lambda\rightarrow 0)$，即K_{IC}后一项等于零(公式(3))，因此裂缝仅需较小的SC−CO_2缝内压力就能延伸。而水基压裂液只能进入大尺度裂缝(图 10)，其缝内压力作用长度为$r-\lambda$，作用距离短，不利于激活微裂缝。另外，由于SC−CO_2可与储层中油水互溶，使得两相界面消失，从而削弱了毛管力的影响，在裂缝尖端形成连续压力降(DPD)[70]，同样也可降低SC−CO_2诱导裂缝扩展所需的缝内净压力，两者共同作用有利于微裂纹的起裂。

3.3 吸附降低裂缝扩展的临界应力

目前，学者研究主要集中于CO_2提高油气采收率(CO_2−EOR)[3]、CO_2提高煤层气采收率(CO_2−ECBM)[78]、CO_2增强型地热系统(CO_2−EGS)[77,79]及CO_2

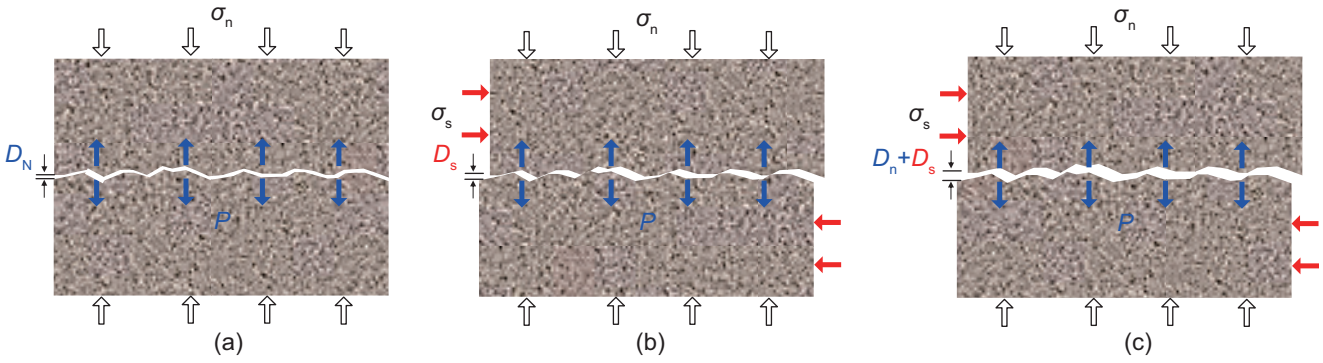

图 8 水力压裂形成的(a)拉伸破坏(I型)、(b)剪切破坏(II型)以及(c)拉伸−剪切混合破坏(I-II型)示意图

Fig. 8 The induced fracture in the form of (a) tensile failure (mode I), (b) shear failure (mode II) and (c) tensile-shear failure (mixed mode I-II)

地质埋存[80]过程中CO_2对岩石力学性质影响。CO_2吸附降低煤岩微裂纹表面能，引起煤岩基质膨胀，导致局部损伤[81]。SC−CO_2作用下煤岩单轴强度和弹性模量要比气态CO_2作用下的小26%和38%，且其降低量与CO_2吸附量之间存在Langmuir关系，即随着CO_2压力的增大其降低速率逐渐减小[78,82]。SC−CO_2作用可降低砂岩的摩擦系数、断裂能和黏聚力，导致其压缩强度和起裂应力分别降低18.82%和21.21%[83]。因此，CO_2与岩石之间的化学—力学耦合作用可弱化力学性质。

水力裂缝扩展是岩石断裂力学问题，裂缝扩展的必要条件是缝内压力克服缝尖的断裂韧性。Griffith[84]根据经典力学和热力学平衡理论提出表面能γ概念，即裂缝在拉应力作用下稳定扩展所需要的功U：

$$U = 2A\gamma \tag{4}$$

式中：A为新裂缝单侧面积，m^2。

Gibbs吸附方程[85]描述了物质表面由于吸附某一活性物质而导致表面能的变化$d\gamma$：

$$d\gamma = -\sum_i \Gamma_i d\mu_i \tag{5}$$

式中：Γ_i为吸附质i的吸附浓度，mg/g；$d\mu_i$为吸附质i的化学势能变化量，J/mol。

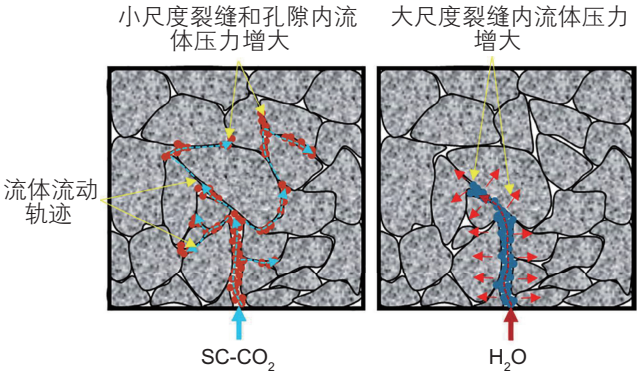

图 10　岩体中SC-CO_2和水流动示意图[77]

Fig. 10　The sketch of SC-CO_2 and water flow in rock[77]

Griffith[84]给出了临界应力改变量$\Delta\sigma_f$和表面能变化量$d\gamma$之间的关系：

$$\Delta\sigma_f = \sqrt{\frac{2Ed\gamma}{\pi r}} \tag{6}$$

气体吸附性能与其分子量、分子直径、单层多层吸附形态等因素相关，且研究表明CO_2的吸附能力大于CH_4[86]。气体吸附在岩石微裂隙表面，降低其表面能，此现象被称为“Rehbindereffect”[87]。吸附导致岩石颗粒间作用力减小或位能降低(粒子间距增大)，随着颗粒间距增大(位能减小到一定程度)裂缝无法愈合。CO_2吸附在未完全断裂的裂隙上，降低固体表面能$d\gamma$(公式(5))，从而降低岩石失稳扩展的临界应力$\Delta\sigma_f$(公式(6))，进而降低外力功(公式(4))。低有效应力条件下，CO_2吸附引起煤岩延伸已有微裂纹或产生平行于层理的新裂缝(图11)，导致煤岩基质不均匀膨胀[88]。由此可见，对于有机质含量高和裂缝发育的油气储层，SC−CO_2压裂或闷井过程中储层有效应力减小，CO_2吸附虽然不会直接诱导新裂缝，但是会促使新裂缝形成。

3.4　局部相变促进裂缝动态扩展

目前非常规油气的CO_2压裂技术和煤层气CO_2相变致裂增透技术逐渐得到工业界的关注。Zhou[40]通过PMMA的压裂实验观察到SC−CO_2具有明显的相变，且发生裂缝动态扩展。CO_2相态由温度场和压力场决定，井底破裂时温度急剧降低，井底CO_2发生超临界态、液态和气态之间的相态变化[18](图12(a))。Yan[89]将SC−CO_2压裂浅层煤岩分为SC−CO_2泵入造缝阶段和停泵后相变造缝阶段，停泵后井筒及裂缝内压力降低至临界压力以下，CO_2发生超临界到气态的相变，此时CO_2迅速膨胀形成冲击载荷进一步延伸裂缝(图12(b))。

不同于浅层煤层气的CO_2相变致裂技术，对于

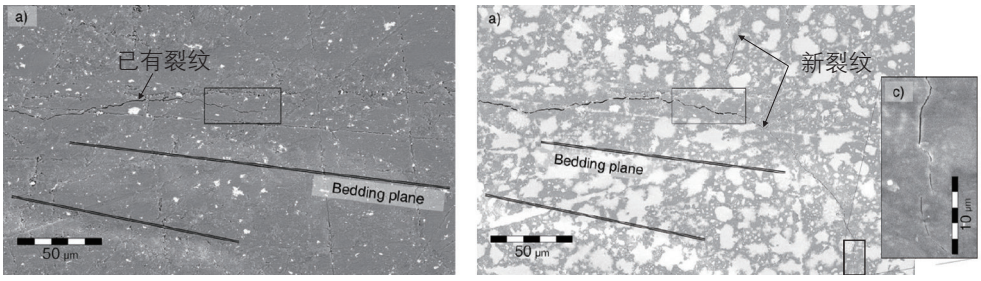

(a) 处理前　　(b) 处理后

图 11　SC-CO_2饱和处理煤岩前后微裂纹分布[88]

Fig. 11　The micro-fracture distribution before and after SC-CO_2 saturation[88]

油气储层来说，地层压力和温度均已超过CO_2的临界条件，宏观主裂缝内SC−CO_2很难产生大范围的相变。由于SC−CO_2压裂动态扩展明显，诱导裂缝的每次间歇式扩展，可看作为缝尖处的一次破裂[90]。裂缝扩展同时缝尖处产生低压甚至真空裂隙，提供了局部CO_2气态条件。SC−CO_2流体迅速膨胀进入该裂隙，导致缝内温度急剧降低(例如初始状态为P=20.69 MPa，T=50 ℃的水和CO_2等焓膨胀到P=0.689 MPa时，水温度未发生变化而CO_2降低了约 200 ℃[25])，该裂隙处发生局部的超临界—液态—气态之间的相变。SC−CO_2压裂可诱导大量分支裂缝，即存在大量裂缝尖端，缝尖的形成往往伴随着CO_2相变。因此，SC−CO_2压裂裂缝每扩展一步，缝尖端就会发生局部相变，所释放的能量以冲击载荷和热应力的形式促进裂缝动态扩展。

4 SC-CO_2压裂机理研究存在的问题及建议

4.1 SC−CO_2诱导裂缝动态起裂

部分SC−CO_2压裂模拟实验由于存在地应力小、排量高、井筒直径大和试件过小等问题，导致SC−CO_2存在明显的动态起裂现象，即试件破裂后注入压力迅速降低，裂缝瞬间扩展到边界。此时，CO_2提供的能量远大于岩体所能吸收的能量，在近井地带产生多裂缝和迂曲裂缝等。因此，实验所得到复杂裂缝并不是裂缝扩展阶段产生，而是动态起裂导致近井地带裂缝迂曲[59]。

为了模拟储层SC−CO_2压裂裂缝的准静态扩展过程，建议SC−CO_2压裂实验采用高围压、低断裂韧性、小直径井筒和割缝(射孔)起裂的条件，从而降低CO_2的能量释放率[91−92]。另外，在试件表面涂抹润滑剂(如凡士林)[18,93]来减轻边界摩擦导致的应力不均匀现象，并尽量增大试件尺寸，从而确保裂缝有效扩展范围。以上措施可以增大裂缝扩展的时间和空间尺度，满足水力压裂相似理论，即物理参数对应和裂缝的准静态扩展。

4.2 SC−CO_2相变促进裂缝扩展

传统水力压裂一般假设岩石线弹性和流体不可压缩，裂缝扩展呈现稳态扩展。SC−CO_2特殊的物性，如低黏度、高滤失、高膨胀性等，导致诱导裂缝特征与扩展机理与常规水力压裂差别较大，因此传统的水力裂缝稳态扩展理论已不再完全适用于SC−CO_2压裂，难以解释缝内CO_2相态变化。

针对油气储层条件下的CO_2相变问题研究，可从多场耦合和微尺度限域效应两方面寻找突破口。多场耦合是针对宏观层面研究，深层油气储层CO_2压裂由于人工裂缝复杂、CO_2物性随温压的变化、CO_2高滤失以及CO_2与储层岩石之间的化学作用，导致其与储层岩石的多场耦合作用强烈。只有掌握SC−CO_2诱导裂缝扩展的耦合规律，才能准确预测裂缝动态扩展过程中的CO_2流体温压的变化。微尺度限域效应是针对微观层面研究，除了温度和压力影响外，微尺度裂纹或孔隙也会影响流体相态变化规律，即流体临界温度和压力随空间尺度发生变化[94]。微尺度限域效应会影响流体结构形态、热力学及动力学行为，传统的PVT

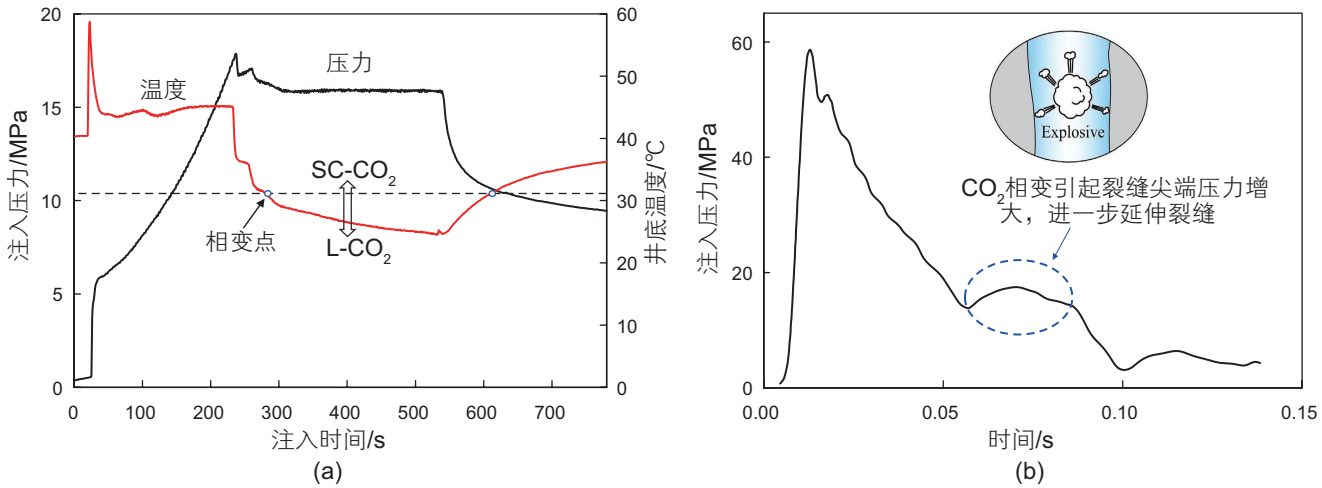

图 12 (a) SC-CO_2压裂注入压力和井底温度变化[18]；(b)CO_2相变导致的压力–时间关系图[89]

Fig. 12 (a) The injection pressure and bottomhole temperature during SC-CO_2 fracturing[18]and (b) the injection pressure versus time during the CO_2 phase change[89]

静态分析方法已经无法解释微纳米尺度孔隙岩石中的流体相态行为[95]。相对于单一的水力裂缝，SC−CO_2 压裂产生大量微尺度裂纹，此时微尺度限域使裂纹内 CO_2 相态变化更为复杂。因此，今后应采用新实验方法、分子模拟等手段，从宏微观方面研究SC−CO_2 压裂裂缝的多场耦合及相态变化规律。

4.3 SC−CO_2 压裂空间裂缝特征定量评价研究

SRV是评价水力压裂改造成功的重要指标，三维(3D)裂缝形态是分析体积裂缝形成机理的重要依据。部分学者通过实验分析 3D裂缝之间的多裂缝干扰机制，指出诱导孔隙压力场分布是其主要影响因素[96−97]。Aimene[98]采用三维各向异性损伤力学模型(ADaM)研究裂缝性储层水力裂缝缝高和井间干扰问题。Daneshy[99]通过解析模型研究三维水力裂缝与天然裂缝之间的相互干扰，分析了天然裂缝空间倾角对剪切破坏的影响。Kizaki[15]研究表明SC−CO_2 压裂易于形成复杂三维裂缝，但没有对裂缝进行量化研究。美国能源局(DOE)于 2015—2018 年开展Wolfcamp页岩储层现场水力压裂试验(HFTS)[100−101]，发现人工裂缝扩展高度有限、支撑剂分布极为不均匀且破碎严重和裂缝复杂且裂缝面形态多样化等现象，认为目前研究完全低估了水力裂缝的复杂程度。相对于常规水力压裂，SC−CO_2 压裂裂缝的复杂程度更高，其中 3D裂缝特征的定量评价是开展研究的基础。

SC−CO_2 的高扩散性导致裂缝扩展以滤失耗散为主，其诱导主裂缝扩展距离短，裂缝宽度小。同时，SC−CO_2 高扩散性导致孔压影响范围大，容易激活主裂缝周围的天然裂缝发生剪切破坏，可以弥补主裂缝扩展距离短的缺点。针对目前非常规储层的开发难点，结合SC−CO_2 压裂裂缝扩展的已有认识，今后应加强含天然裂缝、分层储层及应力等非均质条件下的SC−CO_2 诱导 3D裂缝扩展研究，对裂缝特征进行重构和定量评价，采用扩展有限元、离散元等数值模拟方法量化分析多场耦合影响规律，实现研究尺度的升级。

5 结论

本文综述了目前室内SC−CO_2 压裂实验方法、裂缝起裂扩展特征与机理以及存在的问题，并给出相关建议。本文着重从SC−CO_2 与储层岩石的“热(T)—流(H)—力(M)—化(C)”耦合作用分析SC−CO_2 诱导裂缝破坏机理，主要体现在诱导应力和弱化断裂性质两方面。诱导应力方面包括：SC−CO_2 诱导孔压和热应力(HTM耦合)降低有效应力及诱发剪切破坏，促进I型和I−II混合型裂缝扩展；SC−CO_2 相变(HTM耦合)以冲击载荷和热应力的形式促进裂缝的动态扩展。弱化断裂性质方面包括：零表面张力作用(HM耦合)降低微裂缝扩展的缝内净压力，易于在主裂缝周围形成分支裂缝；SC−CO_2 吸附(CM耦合)降低裂缝扩展的临界应力，减低裂缝形成所需的能量，形成更多的裂缝面积。SC−CO_2 低黏度和高扩散性，导致其与储层岩石之间HTC−M耦合作用强烈，这是SC−CO_2 压裂形成多裂缝的主要原因。

目前，关于SC−CO_2 压裂机理研究，首先要解决压裂模拟的动态起裂问题，增大裂缝扩展时间和空间尺度，确保裂缝扩展的有效性。然后，开展SC−CO_2 三维裂缝扩展实验模拟，对三维裂缝特征进行重构和定量评价。基于实验研究，加强理论模型和数值模拟研究，采用扩展有限元、离散元等数值模拟方法量化分析多场耦合影响，刻画裂缝的温度场和压力场分布，掌握 CO_2 相态分布规律，实现研究尺度的升级。

参考文献

[1] 能源问题. 2100 年全球二氧化碳排放量预测[EB/OL]. [2018−03−07]. http: //euanmearns. com/global-CO_2−emissions-forecast-to−2100/. [Energymatters. Global CO_2 emissions forecast to 2100[EB/OL]. [2018−03−07]]

[2] 王香增, 吴金桥, 张军涛. 陆相页岩气层的CO_2 压裂技术应用探讨[J]. 天然气工业, 2014, 34(01): 64−67. [WANG X Z, WU J Q, ZHANG J T. Applicationof CO_2 fracturing technology for terrestrial shale gas reservoirs[J]. Nat Gas Ind, 2014, 34(01): 64−67.]

[3] JIA B, TSAU J S, BARATI R. A review of the current progress of CO_2 injection EOR and carbon storage in shale oil reservoirs[J]. Fuel, 2019, 236: 404−427.

[4] 才博, 王欣, 蒋廷学, 等. 液态CO_2 压裂技术在煤层气压裂中的应用[J]. 天然气技术, 2007, 1(5): 40−42. [CAI B, WANG X, JIANG X Y, et al. The application of liquid CO_2fracturing in the coalbed methane[J]. Nat Gas Tech, 2007, 1(5): 40−42.]

[5] 刘合, 王峰. 二氧化碳干法压裂技术—应用现状与发展趋势[J]. 石油勘探与开发, 2014, 41(4): 466−472. [LIU H, WANG F. Fracturing with carbon dioxide: Application status and development trend[J]. Petroleum Exploration and Eevelopment, 2014, 41(4): 466−472.

[6] LILLIES A T, KING S R. Sand fracturing with liquid carbon dioxide[C]. In SPE Production Technology Symposium, 8−9 November, Hobbs, New Mexico, 1982, SPE−11341−MS.

[7] MENG S, LIU H, XU J, et al. The evolution and control of fluid phase during liquid CO_2 fracturing[C]. In SPE Asia Pacific Hydraulic Fracturing Conference, 24−26 August, Beijing, China, 2016, SPE−181790−MS.

[8] 孙宝江, 王金堂, 孙文超, 等. 非常规天然气储层超临界CO_2压裂技术基础研究进展[J]. 中国石油大学学报(自然科学版), 2019, 43 (5) : 82−91. [SUN B J, WANG J S, SUN W C, et al. Advance in fundamental research of supercritical CO_2 fracturing technology for unconventional natural gas reservoirs [J]. J China University of Petroleum (Edition of Natural Science) 2019, 43 (5) : 82−91.]

[9] 张强德, 赵万祥, 王法轩. 高能气体压裂技术[J]. 断块油气田, 1994(03): 50−60. [ZHANG D Q, ZHAO W X, WANG F X. The high-energy gas fracturing technology [J]. Fault-Block Oil Gas Field, 1994(03): 50−60.]

[10] 苏伟东, 宋振云, 马得华, 等. 二氧化碳干法压裂技术在苏里格气田的应用[J]. 钻采工艺, 2011(04): 39−44. [SU W D, SONG Z Y, MA D H, et al. Application of CO_2 fracturing technology in SULIGE gas field [J]. Drilling Production Technology, 2011(04): 39−44.]

[11] 杨发, 汪小宇, 李勇. 二氧化碳压裂液研究及应用现状[J]. 石油化工应用, 2014(12): 15−18. [YANG F, WANG X Y, LI Y. Research and application status of CO_2 fracturing fluid [J]. Petrochemical Industry Application, 2014(12): 15−18.]

[12] 雷群, 李宪文, 慕立俊, 等. 低压低渗砂岩气藏CO_2压裂工艺研究与试验[J]. 天然气工业, 2005, 25(4): 113−115. [LEI Q, LI X W, MU L J, et al. Study and test CO_2 fracturing techniques for sand reservoirs with low pressure and permeability[J]. Natur Gas Ind, 2005, 25(4): 113−115.]

[13] 张强德, 王培义, 杨东兰. 储层无伤害压裂技术—液态CO_2压裂[J]. 石油钻采工艺, 2004, 24(4): 47−50. [ZHANG D, WANG P Y, YANG L D. Thereservoir harmless fracturing-liquid CO_2 fracturing[J]. Oil Drilling Production Technology, 2004, 24(4): 47−50.]

[14] KOLLE J J. Coiled-tubing drilling with supercritical carbon dioxide[C]. In SPE/CIM International Conference on Horizontal Well Technology, 6−8 November, Calgary, Alberta, Canada, 2000, SPE−65534−MS.

[15] KIZAKI A, TANAKA H, OHASHI K, et al. Hydraulic fracturing in inada granite and ogino tuff with super critical carbon dioxide[J]. In International Society for Rock Mechanics and Rock Engineering ISRM Regional Symposium−7th Asian Rock Mechanics Symposium, 15−19 October, Seoul, Korea, 2012, ISRM-ARMS7−2012−109.

[16] Li X, FENG Z, HAN G, et al. Breakdown pressure and fracture surface morphology of hydraulic fracturing in shale with H_2O, CO_2 and N_2[J]. Geomech Geophysics for Geo-Energy and Geo-Resources, 2016, 2(2): 63−76.

[17] ZHANG X, LU Y, TANG J, et al. Experimental study on fracture initiation and propagation in shale using supercritical carbon dioxide fracturing[J]. Fuel, 2017, 190: 370−378.

[18] ZHOU D, ZHANG G, PRASAD M, et al. The effects of temperature on supercritical CO_2 induced fracture: An experimental study[J]. Fuel, 2019, 247: 126−134.

[19] ZHOU X, BURBEY T J. Fluid effect on hydraulic fracture propagation behavior: A comparison between water and supercritical CO_2−like fluid[J]. Geofluids, 2014, 14(2): 174–188.

[20] HA S J, CHOO J, YUN T S. Liquid CO_2 fracturing: Effect of fluid permeation on the breakdown pressure and cracking behavior[J]. Rock Mech Rock Eng, 2018, 51(11): 3407−3420.

[21] FANG C, CHEN W, AMRO M. Simulation study of hydraulic fracturing using super critical CO_2 in shale[C]. In International Petroleum Exhibition and Conference, 10−13 November, Abu Dhabi, UAE, 2014, SPE−172110−MS.

[22] WANG J, ELSWORTH D, WU Y, et al. The influence of fracturing fluids on fracturing processes: A comparison between water, oil and SC-CO_2[J]. Rock Mech Rock Eng, 2018, 51(1): 299−313.

[23] WANG D, CHEN M, JIN Y, et al. Effect of fluid compressibility on toughness-dominated hydraulic fractures with leak off [J]. SPE J, 2018, 23(06): 2118−2132, SPE−193995−PA.

[24] LI X, LI G, YU W, et al. Thermal effects of liquid/supercritical carbon dioxide arising from fluid expansion in fracturing[J]. SPE J, 2018, 23(06): 2026−2040, SPE−191357−PA.

[25] MIDDLETON R S, CAREY J W, CURRIER R P, et al. Shale gas and non-aqueous fracturing fluids: Opportunities and challenges for supercritical CO_2[J]. Applied Energy, 2015, 147: 500−509.

[26] WANG H, LI G, ZHU B, et al. Key problems and solutions in supercritical CO_2 fracturing technology[J]. Frontiers in Energy, 1−6.

[27] 张健, 徐冰, 崔明明. 纯液态二氧化碳压裂技术研究综述[J]. 绿色科技, 2014(4): 200−203. [ZHANG J, XU B, CUI M M. Review of fracturing technology of pure liquid carbon dioxide [J]. J Green Science and Technology. 2014(4): 200−203.]

[28] 王海柱, 沈忠厚, 李根生. 超临界CO_2开发页岩气技术[J]. 石油钻探技术, 2011, 39(3): 30−35. [WANG H Z, SHEN Z H, LI G S. Feasibility analysis on shale gas exploitation with supercritical CO_2[J]. Drilling Petroleum Techniques, 2011, 39(3): 30−35.]

[29] ZHOU J, HU N, XIAN X, et al. Supercritical CO_2 fracking for enhanced shale gas recovery and CO_2 sequestration: Results, status and future challenges[J]. Advances in Geo-Energy Research, 2019, 3(2): 207−224.

[30] FU C, LIU N. Waterless fluids in hydraulic fracturing–A Review[J]. J Nat Gas SciEng, 2019, 67: 214−224.

[31] SONG X, GUO Y, ZHANG J, et al. Fracturing with carbon dioxide: From microscopic mechanism to reservoir application[J]. Joule,

2019, 3(8): 1913−1926.

[32] 王香增, 孙晓, 罗攀, 等. 非常规油气CO_2压裂技术进展及应用实践[J]. 岩性油气藏, 2019, 31(02): 4−10. [WANG X Z, SUN X, LUO P, et al. Progress and application of CO_2 fracturing technology for unconventional oil and gas [J]. Lithologic Reservoirs, 2019, 31 (2): 1−7.]

[33] GANDOSSI L. An overview of hydraulic fracturing and other formation stimulation technologies for shale gas production[J]. Eur. Commisison Jt. Res. Cent. Tech. Reports, 2013, 26347.

[34] 唐颖, 唐玄, 王广源, 等. 页岩气开发水力压裂技术综述[J]. 地质通报, 2011, 31(2): 393−399. [TANG Y, TANG X, WANG G Y, et al. Summary of hydraulic fracturing technology in shale gas development [J]. Geological Bulletin of China, 2011, 31(2): 393−399.]

[35] 钱伯章, 李武广. 页岩气井水力压裂技术及环境问题探讨[J]. 天然气与石油, 2013 (1): 48−53. [QIAN B Z, LI W G. A discussion of effects of shale hydraulic fracturing on environment [J]. Nat Gas and Oil, 2013 (1): 48−53.]

[36] 邹才能, 朱如凯, 吴松涛, 等. 常规与非常规油气聚集类型, 特征, 机理及展望——以中国致密油和致密气为例[J]. 石油学报, 2012 (2012 年 02): 173−187. [ZOU C N, ZHU R K, WU S T, et al. Types, characteristics, genesis and prospects of conventional and unconventional hydrocarbon accumulations: Taking tight oil and tight gas in China as an instance[J]. Acta Petrolei Sinica, 2012: 173−187.]

[37] 王良书, 李成, 刘绍文, 等. 塔里木盆地北缘库车前陆盆地地温梯度分布特征[J]. 地球物理学报, 2003, 46(3): 403−407. [WANG S L, LI C, LIU S W, et al. Geotemperaturegradient distribution of Kuqaforeland basin [J]. Chinese J Geophysics, 2003, 46(3): 403−407.]

[38] 陈勉, 庞飞, 金衍. 大尺寸真三轴水力压裂模拟与分析[J]. 岩石力学与工程学报, 2000, 19(S1): 868−872. [CHEN M, PANG F, JIN Y. Experiments and analysis on hydraulic fracturing by a large-size triaxial simulator[J]. Chinese J Rock Mech Eng, 2000, 19(S1): 868−872.]

[39] ZHOU D, ZHANG G, WANG Y, et al. Experimental investigation on fracture propagation modes in supercritical carbon dioxide fracturing using acoustic emission monitoring[J]. Int J Rock Mech Min Sci, 2018, 110: 111−119.

[40] ZHOU D, ZHANG G, ZHAO P, et al. Effects of post-instability induced by supercritical CO_2 phase change on fracture dynamic propagation[J]. J Petro Sci Eng, 2018, 162: 358−366.

[41] SAFARI M R, GANDIKOTA R, MUTLU U, et al. Pulsed fracturing in shale reservoirs: Geomechanical aspects, ductile-brittle transition and field implications[C]. In SPE/AAPG/SEG Unconventional Resources Technology Conference, 12−14 August, Denver, Colorado, USA, 2013, URTEC−1579760−MS.

[42] WARPINSKIN R, SCHMIDT R A, COOPER P W, et al. High-energy gas frac: Multiple fracturing in a wellbore[C]. In 20th U. S. Symposium on Rock Mechanics, 4−6 June, Austin, Texas, 1979, ARMA−79−0143.

[43] ZOBACK M D, KOHI A H. Unconventional reservoir geomechanics[M]. Cambridge University Press, 2019.

[44] ISAKA B L A, RANJITHP G, RATHNAWEERA T D, et al. Testing the frackability of granite using supercritical carbon dioxide: Insights into geothermal energy systems[J]. J CO_2 Utilization, 2019, 34: 180−197.

[45] JIANG Y, QIN C, KANG Z, et al. Experimental study of supercritical CO_2 fracturing on initiation pressure and fracture propagation in shale under different triaxial stress conditions[J]. J Nat Gas Sci Eng, 2018, 55: 382−394.

[46] CHEN Y, NAGAYA Y, ISHIDA T. Observations of fractures induced by hydraulic fracturing in anisotropic granite[J]. Rock Mech Rock Eng, 2015, 48(4): 1455−1461.

[47] WANG L, YAO B, XIE H, et al. CO_2 injection-induced fracturing in naturally fractured shale rocks[J]. Energy, 2017, 139: 1094−1110.

[48] ISHIDA T, DESAKI S, YAMASHITA H, et al. Injection of supercritical carbon dioxide into granitic rock and its acoustic emission monitoring[J]. Procedia Engineering, 2017, 191: 476−482.

[49] SAMPATH K, PERARA M S A, RANJITHP G, et al. Evaluation of superiority of liquid CO_2 as a non-aqueous fracturing fluid for coal seam gas extraction[C]. In 52nd U. S. Rock Mechanics/Geomechanics Symposium, 17−20 June, Seattle, Washington, 2018, ARMA−2018−101.

[50] 王磊, 梁卫国. 超临界CO_2/清水压裂煤体起裂和裂缝扩展试验研究[J]. 岩石力学与工程学报, 2019(A01): 2680−2689. [WANG L, LIANG W. Experimental study on fracture initiation and growth in coal using hydraulic fracturing with SC-CO_2 and water[J]. Chinese J Rock Mech Eng, 2019(A01): 2680−2689]

[51] ZHAO Z, LI X, HE J, et al. A laboratory investigation of fracture propagation induced by supercritical carbon dioxide fracturing in continental shale with interbeds[J]. J Petro Sci Eng, 2018, 166: 739−746.

[52] ZOU Y, LI N, MA X, et al. Experimental study on the growth behavior of supercritical CO_2−induced fractures in a layered tight sandstone formation[J]. J Nat Gas Sci Eng, 2018, 49: 145−156.

[53] 叶亮, 邹雨时, 赵倩云, 等. 致密砂岩储层CO_2压裂裂缝扩展实验研究[J]. 石油钻采工艺, 2018, 40(03): 93−100. [YE L, ZOU Y S, ZHAO Q Y, et al. Experimental research on the CO_2 fracturingfracture propagation laws of high sandstone[J]. Oil Drilling Production Technology. 2018, 40(03): 93−100.]

[54] DENG B, YIN G, LI M, et al. Feature of fractures induced by hydrofracturing treatment using water and L-CO_2 as fracturing fluids in

laboratory experiments[J]. Fuel, 2018, 226: 35−46.

[55] HE J, ZHANGY, LI X, et al. Experimental investigation on the fractures induced by hydraulic fracturing using freshwater and supercritical CO_2 in shale under uniaxial stress[J]. Rock Mech Rock Eng, 1−12.

[56] ALPERN J, MARONE C, ELSWORTH D, et al. Exploring the physicochemical processes that govern hydraulic fracture through laboratory experiments[C]. In 46th U. S. Rock Mechanics/Geomechanics Symposium, 24−27 June 2012, Chicago, Illinois, ARMA−2012−678.

[57] ZHOU D, ZHANG G, et al. Inclined fractures and branches induced by supercritical CO_2: Laboratory study[C]. In 53rd U. S. Rock Mechanics/Geomechanics Symposium, 23−26 June 2019, New York City, New York, ARMA−2019−1822.

[58] CHEN H, HU Y, KANG Y, et al. Fracture initiation and propagation under different perforation orientation angles in supercritical CO_2 fracturing[J]. J Petro Sci Eng, 2019: 106403.

[59] FRASH L P, HAMPTON J, GUTIERREZ M, et al. Patterns in complex hydraulic fractures observed by true-triaxial experiments and implications for proppant placement and stimulated reservoir volumes[J]. J Petro Exploration and Production Tech, 2019, 9(4): 2781−2792.

[60] BISSELL R C, VASCO D W, ATBI M, et al. A full field simulation of the In Salah gas production and CO_2 storage project using a coupled geo-mechanical and thermal fluid flow simulator[J]. Energy Procedia, 2011, 4: 3290−3297.

[61] PERKINS T K, GONZALEZ J A. The effect of thermoelastic stresses on injection well fracturing[J]. SPE J., 1985, 25(01): 78−88, SPE−11332−PA.

[62] SURI A, SHARMA M M. Fracture growth in horizontal injectors[C]. In SPE Hydraulic Fracturing Technology Conference, 19−21 January, The Woodlands, Texas, 2009, SPE−119379−MS.

[63] 王海柱, 李根生, 贺振国, 等. 超临界CO_2岩石致裂机制分析[J]. 岩土力学, 2018, 39(10): 3589−3596. [WANG H Z, LI G S, HE Z G, et al. Analysis of mechanisms of supercritical CO_2 fracturing[J]. Rock and Soil Mechanics, 2018, 39(10): 3589−3596.]

[64] SEGALL P, POLLARD D D. Nucleation and growth of strike slip faults in granite[J]. J Geophys Res: Solid Earth, 1983. 88(B1): 555−568.

[65] WARPINSKI N R, WOLHART S L, WRIGHT C A. Analysis and prediction of microseismicity induced by hydraulic fracturing[C]. In SPE Annual Technical Conference and Exhibition, 30 September−3 October, New Orleans, Louisiana, 2001, SPE−71649−MS.

[66] MCCLURE M W, HORNE R N. An investigation of stimulation mechanisms in enhanced geothermal systems[J]. Int J Rock Mech Min Sci, 2014, 72: 242−260.

[67] ZHANG X, JEFFREY R G. Fluid-driven nucleation and propagation of splay fractures from a permeable fault[J]. Journal of Geophysical Research: Solid Earth, 2016, 121(7): 5257−5277.

[68] BARTON C, MOOS D, TEZUKA K. Geomechanical wellbore imaging: Implications for reservoir fracture permeability[J]. AAPG Bulletin, 2009, 93(11): 1551−1569.

[69] LECAMPION B, BUNGER A, ZHANG X. Numerical methods for hydraulic fracture propagation: A review of recent trends[J]. J Nat Gas Sci Eng, 2018, 49: 66−83.

[70] LIU B L, SUZUKI A, ITO T. Effect of capillary force on performance of shale rock fracturing[C]. In 53rd U. S. Rock Mechanics/Geomechanics Symposium, 23−26 June, New York City, 2019, ARMA−2019−0295.

[71] ESCOBEDO J, MANSOORI G A. Surface tension prediction for pure fluids[J]. AIChE J., 1996, 42(5): 1425−1433.

[72] LEVERETT M. C. Capillary behaviour in porous solids[J]. Trans AIME, 1941, Vol. 142.

[73] GEERTSMA J, DE KLERK F. A rapid method of predicting width and extent of hydraulically induced fractures[J]. J Petrol Tech, 1969, 21(12): 1, 571−1, 581.

[74] WARPINSKI N R. Measurement of width and pressure in a propagating hydraulic fracture[J]. Society of Petroleum Engineers J., 1985, 25(01): 46−54.

[75] JOHNSON E, CLEARY M P. Implications of recent laboratory experimental results for hydraulic fractures[C]. In Low Permeability Reservoirs Symposium, 15−17 April, Denver, Colorado, 1991, SPE−21846−MS.

[76] BERRY M V, DURRANSR F, EVANS R. The calculation of surface tension for simple liquids[J]. J Physics A: General Physics, 1972, 5(1): 166.

[77] ISAKA B L A, RANJITHP G, RATHNAWEERA T D. The use of super-critical carbon dioxide as the working fluid in enhanced geothermal systems (EGSs): A review study[J]. Sustainable Energy Technologies and Assessments, 2019, 36: 100547.

[78] PEREA M S A, RANJITHP G, VIETE D R. Effects of gaseous and super-critical carbon dioxide saturation on the mechanical properties of bituminous coal from the Southern Sydney Basin[J]. Applied Energy, 2013, 110: 73−81.

[79] ISAKA B L A, RANJITHP G, RATHNAWEERA T D, et al. Influence of long-term operation of supercritical carbon dioxide based enhanced geothermal system on mineralogical and microstructurally-induced mechanical alteration of surrounding rock mass[J]. Renewable Energy, 2019, 136: 428−441.

[80] ROHMER J, PLUYMAKERS A, RENARD F. Mechano-chemical interactions in sedimentary rocks in the context of CO_2 storage: Weak acid, weak effects?[J]. Earth-Science Reviews, 2016, 157: 86−110.

[81] PERERA M S A, RANJITHP G, PETER M. Effects of saturation medium and pressure on strength parameters of Latrobe Valley brown coal: Carbon dioxide, water and nitrogen saturations[J]. Energy, 2011, 36(12): 6941−6947.

[82] MASOUDIAN M S, AIREY D W, EL-ZEIN A. Experimental investigations on the effect of CO_2 on mechanics of coal[J]. Int J Coal Geology, 2014, 128: 12−23.

[83] ZHANG G, ZHOU D, WANG P, et al. Influence of supercritical CO_2−water on the micromechanical properties of sandstone[J]. Int J Greenh Gas Control, 2020, 97: 103040.

[84] GRIFFITH A A. VI. The phenomena of rupture and flow in solids[J]. Philosophical Transactions of the Royal Society of London. Series A, containing papers of a mathematical or physical character, 1921, 221(582−593): 163−198.

[85] GIBBS J W. On the equilibrium of heterogeneous substances[J]. American J Sci, 1878 (96): 441−458.

[86] 李树刚, 白杨, 林海飞, 等. CH_4, CO_2 和 N_2 多组分气体在煤分子中吸附热力学特性的分子模拟[J]. 煤炭学报, 2018, 43(09): 114−121. [LI S G, BAI Y, LIN H F, et al. Molecular simulation of adsorption thermodynamics of multicomponent gas CH_4, CO_2 and N_2 in coal [J]. J China Coal Society, 2018, 43(09): 114−121]

[87] REHBINDER P A, SHCHUKINE D. Surface phenomena in solids during deformation and fracture processes[J]. Prog. Surf. Sci., 3, 1972, 97−188.

[88] HOL S, SPIERS C J, PEACH C J. Microfracturing of coal due to interaction with CO_2 under unconfined conditions[J]. Fuel, 2012, 97: 569−584.

[89] YAN H, ZHANG J, ZHOU N, et al. Staged numerical simulations of supercritical CO_2 fracturing of coal seams based on the extended finite element method[J]. J. Nat Gas Sci Eng, 2019, 65: 275−283.

[90] YANG X, ZHANG G, DU X, et al. Measurement and implications of the dynamic fracture width in hydraulic fracturing using FBG strain sensors[C]. In 51st US Rock Mechanics/Geomechanics Symposium. American Rock Mechanics Association, 2017, ARMA−2017−0702.

[91] DE PATER C J, CLEARYM P, QUINN T S, et al. Experimental verification of dimensional analysis for hydraulic fracturing[J]. SPE Production Facilities, 1994, 9(04): 230−238.

[92] BUNGER A P, JDFFERY R G, DETOURNAY E. Application of scaling laws to laboratory-scale hydraulic fractures[C]. In Alaska Rocks 2005, The 40th U. S. Symposium on Rock Mechanics (USRMS), 25−29 June, Anchorage, Alaska, 2005, ARMA−05−818.

[93] GROENENBOOM J, ROMIJN R. Acoustic monitoring of hydraulic fracture growth[J]. First Break, 1997, 15(9): 295−303.

[94] PITAKBUNKATE T, BALBUENA P B, MORIDIS G J, et al. Effect of confinement on pressure/volume/temperature properties of hydrocarbons in shale reservoirs[J]. SPE J, 2016, 21(02): 621−634, SPE−170685−PA.

[95] SALAHSHOOR S, FAHES M, TEODORIU C. A review on the effect of confinement on phase behavior in tight formations[J]. J Nat Gas SciEng, 2018, 51: 89−103.

[96] 周大伟, 张广清, 刘志斌, 等. 致密砂岩多段分簇压裂中孔隙压力场对多裂缝扩展的影响[J]. 石油学报, 2017, 38(7): 830−839. [ZHOU D W, ZHANG G Q, LIU Z B, et al. Influences of pore-pressure field on multi-fracture propagation during the multi-stage cluster fracturing of tight sandstone [J]. Acta Petrolei Sinica, 2017, 38(7): 830−839]

[97] CHANG F F, BARTKO K, DYER S, et al. Multiple fracture initiation in openhole without mechanical isolation: First step to fulfill an ambition[C]. In SPE Hydraulic Fracturing Technology Conference, 4−6 February, The Woodlands, Texas, USA, 2014, SPE−168638−MS.

[98] AIMENE Y, HAMMERQUIST C, OUENES A, et al. 3D anisotropic damage mechanics for modeling interaction between hydraulic and natural fracture planes in a layered rock–application to eagle ford and wolfcamp[C]. In SPE/AAPG/SEG Unconventional Resources Technology Conference, 23−25 July, Houston, Texas, USA, 2018, URTEC−2902985−MS.

[99] DANESHY A. Three-dimensional analysis of interactions between hydraulic and natural fractures[C]. In SPE Hydraulic Fracturing Technology Conference and Exhibition, 5−7 February, The Woodlands, Texas, USA, 2019, SPE−194335−MS.

[100] CIEZOBKA J, COURTIER J, WICKER J. Hydraulic fracturing test site (HFTS)–project overview and summary of results[C]. In SPE/AAPG/SEG Unconventional Resources Technology Conference, 23−25 July, Houston, Texas, USA, 2018, URTEC−2937168−MS.

[101] GALE J F W, ELLIOTT S J, LAUBACH S E. Hydraulic fractures in core from stimulated reservoirs: Core fracture description of HFTS Slant Core, Midland Basin, West Texas[C]. In SPE/AAPG/SEG Unconventional Resources Technology Conference, 23−25 July, Houston, Texas, USA, 2018, URTEC−2902624−MS.

(编辑　马桂霞)